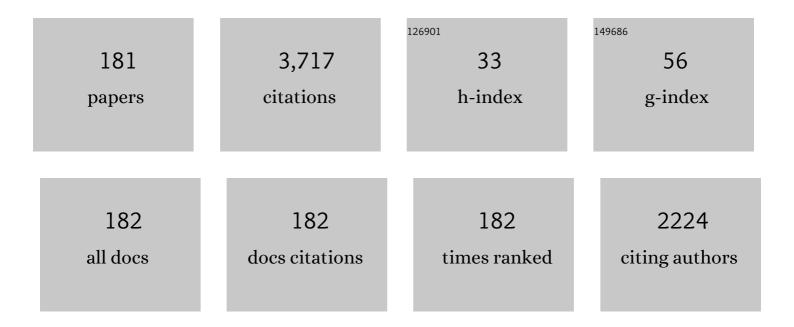
List of Publications by Year in descending order

Source: https://exaly.com/author-pdf/8774752/publications.pdf Version: 2024-02-01



#	Article	IF	CITATIONS
1	Effect of grain boundary on the friction coefficient of pure Fe under the oil lubrication. Tribology International, 2021, 155, 106781.	5.9	8
2	Novel â^'75°C SEM cooling stage: application for martensitic transformation in steel. Microscopy (Oxford, England), 2021, 70, 250-254.	1.5	1
3	Self-accommodation and morphological characteristics of the B33 martensite in Zr–Co–Pd alloys. Journal of Materials Science, 2021, 56, 5899-5909.	3.7	4
4	Effect of Ni Concentrations and C/O Ratios on the Stability of Nonmetallic Inclusions in Ni-Rich Ti-Ni Alloys. Nippon Kinzoku Gakkaishi/Journal of the Japan Institute of Metals, 2021, 85, 162-166.	0.4	0
5	Precipitation Behaviors in Ti–2.3 Wt Pct Cu Alloy During Isothermal and Two-Step Aging. Metallurgical and Materials Transactions A: Physical Metallurgy and Materials Science, 2021, 52, 2760-2772.	2.2	2
6	Superconductivity in Ti67Zr19Nb11.5Sn2.5 shape memory alloy. Physical Review Materials, 2021, 5, .	2.4	0
7	Suppression mechanism of abnormal grain growth by Zr addition in pressless processed Nd-Fe-B sintered magnets. Journal of Alloys and Compounds, 2021, 887, 161244.	5.5	8
8	Tuning martensite transformation behavior and magneto-caloric effect in Ni44Mn36In14Co6 alloy through doping the fifth element Cu. Journal of Alloys and Compounds, 2020, 817, 153150.	5.5	8
9	Effect of C/O Ratio on Phase Change and Stability of Inclusions in Ti–Ni Alloys Fabricated by a Commercial Production Process. Shape Memory and Superelasticity, 2020, 6, 354-364.	2.2	2
10	Elemental Distribution near the Grain Boundary in a Nd–Fe–B Sintered Magnet Subjected to Grain-Boundary Diffusion with Dy <sub>2</sub> 0 <sub>3</sub> . Materials Transactions, 2020, 61, 438-443.	1.2	6
11	Isothermal Martensitic Transformations in an Aged Ni-Rich Ti–Ni Alloy Containing Coherent Ti <sub>3</sub> Ni <sub>4</sub> Particles. Materials Transactions, 2020, 61, 37-41.	1.2	9
12	Effect of Lattice Defects on Tribological Behavior for High Friction Coefficient under TCP Added PAO Lubrication in Nanostructured Steels. ISIJ International, 2020, 60, 1358-1365.	1.4	9
13	Microstructural Characterization of Martensite with Long Period Stacking Order Structure in Hf–Co–Pd Alloy. Materials Transactions, 2020, 61, 27-32.	1.2	0
14	Comparison of <i>In Situ</i> SEM and TEM Observations of Thermoelastic Martensitic Transformation in Ti–Ni Shape Memory Alloy. Materials Transactions, 2020, 61, 2107-2114.	1.2	9
15	Effect of Nonmetallic Inclusions on Fatigue Properties of Superelastic Ti-Ni Fine Wire. Metals, 2019, 9, 999.	2.3	5
16	Microstructure and Martensitic Transformation Behavior in Thermal Cycled Equiatomic CuZr Shape Memory Alloy. Metals, 2019, 9, 580.	2.3	6
17	Effect of Lattice Defects on Tribological Behavior for High Friction Coefficient under TCP added PAO Lubrication in Nanostructured Steels. Tetsu-To-Hagane/Journal of the Iron and Steel Institute of Japan, 2019, 105, 282-289.	0.4	3
18	Characterization of Antiphase Boundary-Like Structure of B33 Martensite in Zr–Co–Pd Alloy. Materials Transactions, 2018, 59, 1567-1573.	1.2	1

#	Article	IF	CITATIONS
19	Influence of Desorption Recombination Temperatures on Microstructure and Coercivity of HDDR-Processed Anisotropic Nd-Fe-B Magnet Powders. Nippon Kinzoku Gakkaishi/Journal of the Japan Institute of Metals, 2018, 82, 121-124.	0.4	0
20	Wide range control of Schottky barrier heights at metal/Ge interfaces with nitrogen-contained amorphous interlayers formed during ZrN sputter deposition. Semiconductor Science and Technology, 2018, 33, 114011.	2.0	1
21	Phase Diagram of near Equiatomic Zr-Pd Alloy. Metals, 2018, 8, 366.	2.3	4
22	Quantification by aberration corrected (S)TEM of boundaries formed by symmetry breaking phase transformations. Ultramicroscopy, 2017, 176, 194-199.	1.9	2
23	Superelasticity and Shape Memory Behavior of NiTiHf Alloys. Shape Memory and Superelasticity, 2017, 3, 168-187.	2.2	30
24	Microstructure and Creep Property in Polycrystalline Ni-based Alloy with Intergranular Intermetallics. Tetsu-To-Hagane/Journal of the Iron and Steel Institute of Japan, 2017, 103, 434-442.	0.4	4
25	Effect of Intergranular Carbides on Creep Strength in Nickel-Based Heat-Resistant Alloys. Materials Transactions, 2017, 58, 52-58.	1.2	4
26	Microstructures of Ta-Inserted SmCo <sub>5</sub> /Fe Nanocomposite Thick Film Magnets. Materials Transactions, 2017, 58, 1351-1355.	1.2	0
27	Antiphase Boundary-Like Structure of B19 Martensite in Ti-Ni-Pd Shape Memory Alloy. Materials Transactions, 2016, 57, 250-256.	1.2	0
28	Imaging of surface spin textures on bulk crystals by scanning electron microscopy. Scientific Reports, 2016, 6, 37265.	3.3	8
29	Creep strengthening by lath boundaries in 9Cr ferritic heat-resistant steel. Philosophical Magazine Letters, 2016, 96, 76-83.	1.2	33
30	Enhancement of ductility in Fe-Co based alloys by substitution of Pd. Journal of Alloys and Compounds, 2016, 682, 124-131.	5.5	5
31	Precipitation Behavior During Aging in α Phase Titanium Supersaturated with Cu. Metallurgical and Materials Transactions A: Physical Metallurgy and Materials Science, 2016, 47, 1544-1553.	2.2	6
32	Morphological and chemical analysis of bainite in Cu–17Al–11Mn (at.%) alloys by using orthogonal FIB-SEM and double-EDS STEM. Microscopy (Oxford, England), 2016, 65, 243-252.	1.5	5
33	In situ scanning electron microscopy study of the thermoelastic martensitic transformation in Ti–Ni shape memory alloy. Acta Materialia, 2016, 103, 352-360.	7.9	47
34	Electrical and structural properties of group-4 transition-metal nitride (TiN, ZrN, and HfN) contacts on Ge. Journal of Applied Physics, 2015, 118, .	2.5	16
35	Shape Memory Response of Polycrystalline NiTi12.5Hf Alloy: Transformation at Small Scales. Shape Memory and Superelasticity, 2015, 1, 387-397.	2.2	15
36	Effect of Cold-working and Mo Addition on Creep Behavior in High Mn Austenitic Stainless Steels. Tetsu-To-Hagane/Journal of the Iron and Steel Institute of Japan, 2015, 101, 51-58.	0.4	1

#	Article	IF	CITATIONS
37	Determination of the atomic width of an APB in ordered CoPt using quantified HAADF-STEM. Journal of Alloys and Compounds, 2015, 644, 570-574.	5.5	15
38	Novel long-period stacking-ordered structure of martensite in zirconium–cobalt–palladium alloys. Philosophical Magazine Letters, 2015, 95, 21-29.	1.2	2
39	The effect of thermal cycling on the martensitic transformation in equiatomic CuZr shape memory alloy. Journal of Alloys and Compounds, 2015, 653, 591-595.	5.5	5
40	Crystallography and morphology of antiphase boundary-like structure induced by martensitic transformation in Ti–Pd–Fe alloy. Journal of Alloys and Compounds, 2015, 618, 527-532.	5.5	2
41	Role of an interlayer at a TiN/Ge contact to alleviate the intrinsic Fermi-level pinning position toward the conduction band edge. Applied Physics Letters, 2014, 104, .	3.3	28
42	Ductility enhancement in Co–Fe–Ni alloys by microstructural control. Intermetallics, 2014, 52, 124-130.	3.9	2
43	Effects of Ni concentration and aging conditions on multistage martensitic transformation in aged Ni-rich Ti–Ni alloys. Acta Materialia, 2014, 69, 17-29.	7.9	65
44	Antiphase boundary-like structure of B19′ martensite via R-phase transformation in Ti–Ni–Fe alloy. Journal of Alloys and Compounds, 2014, 586, 87-93.	5.5	13
45	In situSEM studies of the transformation sequence of multistage martensitic transformations in aged Ti-50.8 at.% Ni alloys. Philosophical Magazine, 2013, 93, 2279-2296.	1.6	15
46	Quantitative microstructure analyses upon multistage martensitic transformation in an aged Ti–50.8at.% Ni alloy. Journal of Alloys and Compounds, 2013, 577, S268-S273.	5.5	6
47	HAADF-STEM studies of athermal and isothermal ï‰-phases in β-Zr alloy. Journal of Alloys and Compounds, 2013, 577, S713-S716.	5.5	16
48	Enhancement of ductility in B2-type Zr–Co–Ni alloys with deformation-induced martensite and microcrack formation. Intermetallics, 2013, 36, 45-50.	3.9	20
49	Microstructure of high coercivity Nd–Fe–Co–Ga–B hot-deformed magnet improved by the Dy diffusion treatment. Journal of Alloys and Compounds, 2013, 557, 1-4.	5.5	42
50	Electron Microscopy Study of Preferential Variant Selection in CoPt Alloy Ordered under a Magnetic Field. Materials Transactions, 2013, 54, 1715-1718.	1.2	3
51	Transmission Electron Microscopy of Twins in 10M Martensite in Ni–Mn–Ga Ferromagnetic Shape Memory Alloy. Materials Transactions, 2012, 53, 902-906.	1.2	21
52	Development of Ductile B2-Type Fe–Co Based Alloys. Materials Transactions, 2012, 53, 1826-1828.	1.2	8
53	Controlling grain boundary character distribution of high-temperature B2 phase in Ti–Ni–Fe alloy. Intermetallics, 2012, 31, 65-71.	3.9	9
54	Self-accommodation of B19′ martensite in Ti–Ni shape memory alloys – Part I. Morphological and crystallographic studies of the variant selection rule. Philosophical Magazine, 2012, 92, 2215-2233.	1.6	83

#	Article	IF	CITATIONS
55	Self-accommodation of B19′ martensite in Ti–Ni shape memory alloys – Part II. Characteristic interface structures between habit plane variants. Philosophical Magazine, 2012, 92, 2234-2246.	1.6	43
56	Self-accommodation of B19′ martensite in Ti–Ni shape memory alloys. Part III. Analysis of habit plane variant clusters by the geometrically nonlinear theory. Philosophical Magazine, 2012, 92, 2247-2263.	1.6	52
57	Hydrogen permeability and microstructure of rapidly quenched Nb–TiNi alloys. Journal of Alloys and Compounds, 2011, 509, S790-S793.	5.5	13
58	Enhancement of ductility in B2-type Zr–Co–Pd alloys with martensitic transformation. Intermetallics, 2011, 19, 894-899.	3.9	30
59	Coercivity enhancement of Dy-coated Nd-Fe-B flakes by crystallization. Journal of Applied Physics, 2011, 109, 07A701.	2.5	7
60	Morphology and Crystallography of Martensite Plate with Long Period Stacking Structure in Ti-Pd Shape Memory Alloy. Materials Transactions, 2011, 52, 2016-2021.	1.2	4
61	Microstructure of Nd-Rich Grain Boundary Phase in Die-Upset Nd-Fe-Co-Ga-B Magnet. Materials Transactions, 2011, 52, 2239-2244.	1.2	8
62	Deformation structure in ductile B2-type Zr–Co–Ni alloys with martensitic transformation. Journal of Materials Science, 2011, 46, 4221-4227.	3.7	26
63	Transmission electron microscopy of antiphase boundary-like structure of B19′ martensite in Ti–Ni shape memory alloy. Acta Materialia, 2011, 59, 133-140.	7.9	22
64	Quantitative three-dimensional analysis of Ni4Ti3 precipitate morphology and distribution in polycrystalline Ni–Ti. Acta Materialia, 2011, 59, 1780-1789.	7.9	45
65	Hydrogen permeation in rapidly quenched amorphous and crystallized Nb20Ti40Ni40 alloy ribbons. International Journal of Hydrogen Energy, 2011, 36, 1784-1792.	7.1	30
66	Microstructure Analysis of High Coercivity PLD-Made Nd-Fe-B Thick-Film Improved by Tb-Coating-Diffusion Treatment. Materials Transactions, 2010, 51, 1939-1943.	1.2	12
67	Materials Separation from Pulverized Waste Printed Circuit Boards. Journal of Environment and Engineering, 2010, 5, 383-388.	0.2	4
68	Structure, conductivity and mechanical properties of non-equilibrium copper-based crystalline alloy nano-composites. Intermetallics, 2010, 18, 1860-1863.	3.9	3
69	Micromechanical Testing of Nanostructured NbTiNi Hydrogen Permeation Membranes. Materials Research Society Symposia Proceedings, 2009, 1224, 1.	0.1	0
70	Techniques to separate metal from waste printed circuit boards from discarded personal computers. Journal of Material Cycles and Waste Management, 2009, 11, 42-54.	3.0	86
71	Microstructure analysis of Ndâ€Feâ€B sintered magnets improved by Tbâ€metal vapour sorption. Journal of Microscopy, 2009, 236, 104-108.	1.8	34
72	Interfacial characterisation in Al–20 vol%SiC <sub>p</sub> explosively compacted composite. Materials Science and Technology, 2009, 25, 108-110.	1.6	2

#	Article	IF	CITATIONS
73	Crystallization and microstructure changes in rapidly solidified Nb20Ti40Ni40 hydrogen permeation alloy. Journal of Alloys and Compounds, 2009, 485, 773-777.	5.5	11
74	Ductility Enhancement in B2-Type Zr-Co-Ni Alloys with Martensitic Transformation. Materials Transactions, 2009, 50, 2335-2340.	1.2	29
75	Internal Defects of B19' Martensite via R-Phase in Ti-Ni-Fe and Thermally Cycled Ti-Ni Alloys. Materials Transactions, 2009, 50, 1219-1224.	1.2	6
76	Influence of Heating Temperature on Interface Separation Behavior between Ti-20 mol% Al Alloy and High Carbon Steel. Materials Transactions, 2009, 50, 2005-2010.	1.2	2
77	PLD of X7R for thin film capacitors. Applied Surface Science, 2008, 254, 2638-2641.	6.1	5
78	Crystallography and morphology of twins in equiatomic TiPt martensite. Materials Science and Technology, 2008, 24, 884-889.	1.6	22
79	Electron Microscopy Study of Eutectic Structure in Nb-Ti-X and Nb-Zr-X (X = Co, Ni) Hydrogen Permeation Alloys. Materials Transactions, 2008, 49, 2208-2213.	1.2	8
80	Crystallography and Morphology of Antiphase Boundary-Like Structure Induced by Martensitic Transformation in Ti-Pd Shape Memory Alloy. Materials Transactions, 2008, 49, 461-465.	1.2	27
81	Interface Separation Phenomenon in Ti-20mol%Al Alloy/Iron Material Joints. Tetsu-To-Hagane/Journal of the Iron and Steel Institute of Japan, 2008, 94, 251-257.	0.4	4
82	High-angle annular dark field scanning transmission electron microscopy of the antiphase boundary in a rapidly solidified B2 type TiPd compound. Philosophical Magazine Letters, 2007, 87, 59-64.	1.2	13
83	Synthesis Method of Nanomaterials by Pulsed Plasma in Liquid. Journal of Nanoscience and Nanotechnology, 2007, 7, 3157-3159.	0.9	38
84	Application of Ni-free Ti-Mo-Sn shape memory alloys to medical tools. Transactions of the Materials Research Society of Japan, 2007, 32, 639-642.	0.2	0
85	Effects of Sn Content and Aging Conditions on Superelasticity in Biomedical Ti–Mo–Sn Alloys. Materials Transactions, 2006, 47, 513-517.	1.2	29
86	Effect of Heat Treatment Atmosphere on Multistage R-Phase Transformation in an Aged Ti–51.0 at%Ni Alloy. Materials Transactions, 2006, 47, 645-649.	1.2	8
87	High maneuverability guidewire with functionally graded properties using new superelastic alloys. Minimally Invasive Therapy and Allied Technologies, 2006, 15, 204-208.	1.2	9
88	Effect of Bending Work on Liquid Zinc Induced Cracking. Journal of High Temperature Society, 2006, 32, 130-136.	0.1	0
89	Fabrication of TiNi Shape Memory Alloys by Laser Atomization Process. Journal of High Temperature Society, 2006, 32, 230-235.	0.1	0
90	Dislocation Structure in Rapidly Solidified Mg <sub>97</sub> Zn <sub>1</sub> Y <sub>2</sub> Alloy with Long Period Stacking Order Phase. Materials Transactions, 2005, 46, 361-364.	1.2	106

#	Article	IF	CITATIONS
91	Variation of long-period stacking order structures in rapidly solidified Mg97Zn1Y2 alloy. Materials Science & Engineering A: Structural Materials: Properties, Microstructure and Processing, 2005, 393, 269-274.	5.6	313
92	Diffusion of carbon and titanium in Î <sup>3</sup> -iron in a magnetic field and a magnetic field gradient. Journal of Materials Science, 2005, 40, 3191-3198.	3.7	90
93	Interface Microstructures of SPCC/A5052/SUS304 Produced using Resistance Spot Welding. Materia Japan, 2005, 44, 967-967.	0.1	0
94	Interaction between Long Period Stacking Order Structure and Deformation Twinin Mg-Y-Zn Alloy. Materia Japan, 2005, 44, 994-994.	0.1	0
95	Microstructure of Martensite in Ti-Ni-Fe Alloy via R Phase Transformation. Materia Japan, 2005, 44, 995-995.	0.1	0
96	Application of the CSL Model to Deformation Twin Boundary in B2 Type TiNi Compound. Materials Research Society Symposia Proceedings, 2004, 842, 269.	0.1	0
97	Effect of Heat Treatment Conditions on Multistage Martensitic Transformation in Aged Ni-rich Ti-Ni Alloys. Materials Research Society Symposia Proceedings, 2004, 842, 227.	0.1	0
98	Interaction between long period stacking order phase and deformation twin in rapidly solidified Mg97Zn1Y2 alloy. Materials Science & Engineering A: Structural Materials: Properties, Microstructure and Processing, 2004, 386, 447-452.	5.6	156
99	Interfacial Microstructures and Bonding Strength between Aluminum Nitride and Silver Brazing Filler Metals Containing Various Active Elements. Journal of the Ceramic Society of Japan, 2004, 112, 305-310.	1.3	3
100	Shape Memory Properties of Biomedical Ti-Mo-Ag and Ti-Mo-Sn Alloys. Materials Transactions, 2004, 45, 1096-1100.	1.2	138
101	Shape Memory and Mechanical Properties of Biomedical Ti-Sc-Mo Alloys. Materials Transactions, 2004, 45, 1101-1105.	1.2	61
102	Effect of Heat-Treatment on Metallic Collection for Used Printed Circuit Board. Journal of High Temperature Society, 2004, 30, 62-66.	0.1	0
103	Effect of a modified deep-fat fryer on chemical and physical characteristics of frying oil. JAOCS, Journal of the American Oil Chemists' Society, 2003, 80, 163-166.	1.9	15
104	Pulverization of waste printed circuit boards. Journal of Material Cycles and Waste Management, 2003, 5, 137-142.	3.0	6
105	Reduction of droplet of tantalum oxide using double slit in pulsed laser deposition. Vacuum, 2003, 70, 47-52.	3.5	10
106	Fabrication of NiTi intermetallic compound by a reactive gas laser atomization process. Materials Science & Engineering A: Structural Materials: Properties, Microstructure and Processing, 2003, 356, 122-129.	5.6	16
107	The PLD of BaTiO3 target produced by SPS and its electrical properties for MLCC application. Materials Science and Engineering B: Solid-State Materials for Advanced Technology, 2003, 103, 128-134.	3.5	14
108	Production of High Strength Mg <sub>97</sub> Zn <sub>1</sub> Y <sub>2</sub> Alloy by Using Mechanically Alloyed MgH <sub>2</sub> Powder. Materials Transactions, 2003, 44, 440-444.	1.2	3

#	Article	IF	CITATIONS
109	Experimental Consideration of Multistage Martensitic Transformation and Precipitation Behavior in Aged Ni-Rich Ti-Ni Shape Memory Alloys. Materials Transactions, 2003, 44, 2631-2636.	1.2	68
110	Fabrication of NiTi Intermetallic Compound Powder by a Reactive Gas Atomization Process using a Laser. Funtai Oyobi Fummatsu Yakin/Journal of the Japan Society of Powder and Powder Metallurgy, 2003, 50, 657-663.	0.2	3
111	Formation of Droplets on Thin Film Surface in Pulsed Laser Deposition Using Metal Targets. Yosetsu Gakkai Ronbunshu/Quarterly Journal of the Japan Welding Society, 2003, 21, 338-343.	0.5	4
112	Martensitic Transformation in Ti-Rich Ti-Pd Shape Memory Alloys. Materials Transactions, 2002, 43, 908-915.	1.2	11
113	Combination and Interface Structure of 9R Martensite Plate Variants in Ti <sub>50.0</sub> Pd <sub>43.0</sub> Fe <sub>7.0</sub> Shape Memory Alloy. Materials Transactions, 2002, 43, 902-907.	1.2	6
114	The effect of 5 mass% O3 gas on PLD of tantalum oxide. Applied Surface Science, 2002, 189, 1-6.	6.1	4
115	Crystallization of tantalum oxide formed by PLD. Surface and Coatings Technology, 2002, 149, 1-6.	4.8	13
116	Effect of Zr and Ta Inserts on Bonding Strength and Interfacial Microstructures of Ti/Steel Clads ISIJ International, 2002, 42, 645-650.	1.4	6
117	FABRICATION OF HYDROXYAPATITE/Ti COMPOSITES BY UNDERWATER-SHOCK COMPACTION. , 2001, , .		0
118	FABRICATION OF POROUS TITANIUM COMPOSITE FOR MEDICAL IMPLANTS BY EXPLOSIVE COMPACTION. , 2001, , .		0
119	Fabrication of Mo/Cu Functionally Graded Material by Underwater-Shock Compaction. , 2001, , .		0
120	A New Electrochemical Method To Prepare Mesoporous Titanium(IV) Oxide Photocatalyst Fixed on Alumite Substrate. Journal of Physical Chemistry B, 2000, 104, 4204-4209.	2.6	96
121	Effect of Heat Treatment on Bonding Characteristics and Interfacial Microstructures in Explosively Welded Ti/SUS430 Stainless Steel Clad. Tetsu-To-Hagane/Journal of the Iron and Steel Institute of Japan, 1999, 85, 340-345.	0.4	10
122	Sliding wear characteristics of Co-based overlay weld metal with dispersed boride particles. Welding International, 1999, 13, 123-132.	0.7	0
123	Microstructure of Mo powders sintered with Ni and Ni3Al powders Funtai Oyobi Fummatsu Yakin/Journal of the Japan Society of Powder and Powder Metallurgy, 1999, 46, 1221-1225.	0.2	3
124	High-temperature oxidation behaviour of laser-clad NiCrAlY. Welding International, 1998, 12, 859-866.	0.7	0
125	Improvement of wear resistance of a laser-sprayed Ti-N coating by laser remelting. Welding International, 1998, 12, 635-641.	0.7	0
126	Recrystallization and Related Phenomena. The Influence of Cold Rolling Reduction on r-value and Recrystallization Behavior in Fe-36Ni Alloy ISIJ International, 1998, 38, 640-646.	1.4	5

#	Article	IF	CITATIONS
127	Elastic Constants of Zirconia Single Crystals Determined by X-ray Measurements for Polycrystals. Materials Transactions, JIM, 1998, 39, 268-274.	0.9	14
128	Type II Twin Boundary Structure of Martensite in Ti-Ni and Ti-Pd Shape Memory Alloys. Materia Japan, 1998, 37, 386-386.	0.1	0
129	Microstructure Dependence of Compactibility of Rapidly Solidified Ti-Rich TiAl Alloy Powders Produced by Plasma Rotating Electrode Process. Materials Transactions, JIM, 1997, 38, 334-343.	0.9	13
130	Phase Transformation and Crystal Structures of Ti <sub>2</sub> Ni <sub>3</sub> Precipitates in Ti–Ni Alloys. Materials Transactions, JIM, 1997, 38, 277-284.	0.9	42
131	Transmission electron microscopy of twins in martensite in Tiî—,Pd shape memory alloy. Acta Materialia, 1997, 45, 4847-4853.	7.9	46
132	B1-type and WC-type phase bulk bodies of tantalum nitride prepared by shock and static compressions. Physica B: Condensed Matter, 1997, 239, 13-15.	2.7	36
133	Diffusion Barrier Effect of TiC Layer Formed at the Bonding Interface and Bonding Characteristics of an Explosively Welded Ti/SUS420J1 Stainless Steel Clad by Heat Treatment. Tetsu-To-Hagane/Journal of the Iron and Steel Institute of Japan, 1997, 83, 736-741.	0.4	5
134	Effect of the Heat Treatments to Microstructures of Low Pressure Plasma Sprayed CoNiCrAlYTa Coating Hyomen Gijutsu/Journal of the Surface Finishing Society of Japan, 1996, 47, 784-789.	0.2	0
135	Diffusion Barrier Effect of Carbide Layer on Bonding Characteristics of Ti/Steel Clad. Materials Research Society Symposia Proceedings, 1996, 458, 363.	0.1	3
136	Phase Transformations and Crystallography of Twins in Martensite in Ti-Pd Alloys. Materials Research Society Symposia Proceedings, 1996, 459, 375.	0.1	2
137	Effect of Initial Microstructure on the Compatibility of Rapidly Solidified Ti-Rich TiAl Powder. Materials Research Society Symposia Proceedings, 1996, 460, 45.	0.1	Ο
138	Specimen Preparation for Transmission Electron Microscopy of Twins in B19′ Martensite of Ti–Ni Shape Memory Alloys. Materials Transactions, JIM, 1996, 37, 210-217.	0.9	21
139	Formation of Nonequilibrium Phases at Collision Interface in an Explosively Welded Ti/Ni Clad. Materials Transactions, JIM, 1995, 36, 1338-1343.	0.9	31
140	Bonding characteristics and diffusion barrier effect of the TiC phase formed at the bonding interface in an explosively welded titanium/high- carbon steel clad. Journal of Phase Equilibria and Diffusion, 1995, 16, 411-415.	0.3	30
141	Electron Microscopy Studies of Bonding Interface in Explosively Welded Ti/Steel Clads ISIJ International, 1995, 35, 217-219.	1.4	55
142	Anomalous shock compression behavior of yttriaâ€doped tetragonal zirconia. Journal of Applied Physics, 1995, 77, 5069-5076.	2.5	26
143	Fabrication of highâ€strength steel fibre reinforced metal matrix composites by explosive bonding and their tensile properties. Welding International, 1995, 9, 179-184.	0.7	1
144	Experimental conditions for fabrication of multilayered metal base composites by singleâ€shot explosive welding. Welding International, 1995, 9, 116-120.	0.7	2

#	Article	IF	CITATIONS
145	High resolution electron microscopy studies of twin boundary structures in B19′ martensite in the Ti-Ni shape memory alloy. Acta Metallurgica Et Materialia, 1995, 43, 1229-1234.	1.8	68
146	Electron microscopy studies of twin morphologies in B19′ martensite in the Ti-Ni shape memory alloy. Acta Metallurgica Et Materialia, 1995, 43, 1219-1227.	1.8	145
147	Effects of particle size of carbide powder and silica sand on abrasive wear resistance of an overlay composite alloy. Welding International, 1994, 8, 23-29.	0.7	3
148	Experimental Conditions for the Fabrication of Multilayered Metal Base Composite Made by Single-Shot Explosive Welding Technique Yosetsu Gakkai Ronbunshu/Quarterly Journal of the Japan Welding Society, 1994, 12, 363-367.	0.5	1
149	Microstructural modifications in an explosively welded Ti/Ti clad material: I. Bonding interface. Metallurgical and Materials Transactions A - Physical Metallurgy and Materials Science, 1993, 24, 735-742.	1.4	35
150	Microstructural modifications in an explosively welded Ti/Ti clad material: II. Deformation structures around bonding interface. Metallurgical and Materials Transactions A - Physical Metallurgy and Materials Science, 1993, 24, 743-750.	1.4	8
151	Joining of Chromized Carbon-Steel and Si <sub>3</sub> N <sub>4</sub> . Journal of the Ceramic Society of Japan, 1993, 101, 1363-1368.	1.3	0
152	Fabrication and Some Mechanical Properties of SiC Whisker-Reinforced Si <sub>3</sub> N <sub>4</sub> Composites Utilizing Underwater-Shock Pressure. Journal of the Ceramic Society of Japan, 1993, 101, 445-450.	1.3	0
153	Explosive Compaction of Silicon Nitride Powder without Additives using a Water Pressure Medium. Journal of the Ceramic Society of Japan, 1992, 100, 1230-1234.	1.3	3
154	Electron microscopy studies of Ti - 47 at. % Al powder produced by plasma rotating electrode process. Scripta Metallurgica Et Materialia, 1992, 27, 335-340.	1.0	17
155	Tem Specimen Preparation of Tial Alloy Powders Produced by Plasma Rotating Electrode Process. Materials Research Society Symposia Proceedings, 1991, 254, 185.	0.1	3
156	Synthesis and morphological aspects of AlN whiskers from Al powders obtained by spark discharged process Zairyo/Journal of the Society of Materials Science, Japan, 1990, 39, 1347-1352.	0.2	0
157	Origin of the silver doping effects on superconducting oxide ceramics. Applied Physics Letters, 1990, 56, 1585-1587.	3.3	49
158	Magnetic Tape Recorder with a Reproducing Head Using Parametric Oscillation for Low Frequency. IEEE Translation Journal on Magnetics in Japan, 1989, 4, 107-113.	0.1	4
159	Effect of Heat Treatment on Tensile Strength of Explosively-Welded Maraging Steel/Al and Maraging Steel/Ti Multilayered Composites. Nippon Kinzoku Gakkaishi/Journal of the Japan Institute of Metals, 1989, 53, 1268-1275.	0.4	6
160	Formation of Transformation Textures and Plastic Anisotropy in Hot-rolled Steel Sheets. Tetsu-To-Hagane/Journal of the Iron and Steel Institute of Japan, 1989, 75, 941-947.	0.4	3
161	Electron microscopy studies of the "Premartensitic―transformations in an aged Ti-51 at%Ni shape memory alloy. Metallography, 1988, 21, 255-273.	0.4	56
162	Electron microscopy studies of the martensitic transformation in an aged Ti-51at%Ni shape memory alloy. Metallography, 1988, 21, 275-291.	0.4	84

#	Article	IF	CITATIONS
163	Explosive consolidation of titanium powder with a pressure medium. Scripta Metallurgica, 1988, 22, 213-217.	1.2	13
164	Improvement of superplasticity of Zn-22Al pre-alloy powder by the use of rapid solidification technique and heat-treatment method Funtai Oyobi Fummatsu Yakin/Journal of the Japan Society of Powder and Powder Metallurgy, 1988, 35, 91-95.	0.2	0
165	Thermal Stability and Mechanical Properties of Explosive-Welded SUS304 Steel Wire Mesh/Al Composite. Nippon Kinzoku Gakkaishi/Journal of the Japan Institute of Metals, 1988, 52, 826-833.	0.4	5
166	Electron microscopy studies of precipitation processes in near-equiatomic TiNi shape memory alloys. Materials Science and Engineering, 1987, 93, 191-203.	0.1	45
167	Further electron microscopy studies of the Ti11 Ni14 phase in an aged Tiî—,52at%Ni shape memory alloy. Scripta Metallurgica, 1986, 20, 899-904.	1.2	60
168	Phase transformations in a Ti50Ni47.5Fe2.5 shape memory alloy. Metallography, 1986, 19, 99-113.	0.4	27
169	Electron microscopy studies of the Ti11Ni14 phase in an aged Ti-52.0at%Ni shape memory alloy. Scripta Metallurgica, 1985, 19, 983-987.	1.2	25
170	Effect of Carbide Forming Elements on the Mechanical Properties of Continuously Annealed Extra-low-carbon Steel Sheets. Transactions of the Iron and Steel Institute of Japan, 1984, 24, 838-846.	0.2	7
171	All-round shape memory effect in Ni-rich TiNi alloys generated by constrained aging. Scripta Metallurgica, 1984, 18, 1293-1298.	1.2	173
172	Effect of heat treatment on the all-round shape memory effect in Ti-5lat%Ni. Scripta Metallurgica, 1984, 18, 1299-1302.	1.2	45
173	Electron microscopy studies of the all-around shape memory effect in a Ti-51.0 at .%Ni alloy. Scripta Metallurgica, 1984, 18, 1389-1394.	1.2	62
174	Production Technology and Mechanical Properties of High Strength Hot Rolled Steel Sheets. Tetsu-To-Hagane/Journal of the Iron and Steel Institute of Japan, 1982, 68, 1290-1296.	0.4	1
175	Spheroidization of Manganese Sulfide Inclusion during Heating and Its Effect on Hydrogen Induced Cracking in Rolled Steel. Tetsu-To-Hagane/Journal of the Iron and Steel Institute of Japan, 1981, 67, 1533-1541.	0.4	4
176	Effects of Hot-rolling Conditions on Austenite Grain Size and Mechanical Properties of Hot-rolled Coil for High Test Line Pipe. Tetsu-To-Hagane/Journal of the Iron and Steel Institute of Japan, 1977, 63, 1116-1125.	0.4	2
177	Structure-Activity Studies of Pyrrolnitrin Analogues. Chemical and Pharmaceutical Bulletin, 1970, 18, 1414-1425.	1.3	13
178	Secondary Recrystallization in Iron-Germanium Alloys. Transactions of the Japan Institute of Metals, 1964, 5, 254-258.	0.5	0
179	Explosive Welding of ZrTiCuNiBe Bulk Metallic Glass to Crystalline Cu Plate. Materials Science Forum, 0, 673, 119-124.	0.3	14
180	Analysis of Stacking Structure and Morphology in Ti50(Ptx, Ir50-x) Martensite by Hrtem and		0

HAADF-Stem. , 0, , 659-662.

#	Article	IF	CITATIONS
181	Transmission Electron Microscopy of Antiphase Boundary-Like Structure Induced by Displacive Transformation in Ti-Pd Shape Memory Alloy. , 0, , 305-309.		0